

Design and Implementation of a New Electronic Technique for Real-Time Correction of Parallax/Lag and Air-condition Noises in Airborne Magnetic Data

K.G. Abdel-Kader¹, A.A.M. Ismail², F.A.S. Soliman³, A.S.S. El-Kabbani⁴,
A.Yahya⁵ and A.M. Abdel-Maksood⁶

¹ South Cairo Electricity Distribution Co., Ministry of Electricity and Renewable Energy, Egypt,

^{2,3,6} Exploration Sector, Nuclear Materials Authority, P.O. Box 530, Maadi-11728, Cairo, Egypt,

^{4,5} Department of Electrical Engineering, Faculty of Eng., Al-Azhar University, Nasr City, Cairo-11371, Egypt.

¹khasdasd2000@gmail.com, ²elshayatatef@yahoo.com,
³fouad.saad.soliman@gmail.com, ⁴ahmed_safwat@yahoo.com,
⁵ahmed_yahya_1@yahoo.com, ⁶ashrafmosleh1@gmail.com

Abstract

Recent developments in airborne magnetic detection systems have made it possible to detect much small magnetic objects such as unexploded ordnance. However, the data sets are extremely large and the measurements must be processed and interpreted. Therefore, there is an increasing need for a fully automatic processing and interpretation techniques that can be used to make decisions regarding the nature of the source in real time. So, the aim of the present paper is to shed further light on the real time correction of parallax/Lag -and air-condition-noises in airborne magnetic data acquisition. A novel electronic technique, based on micro-controllers design and implementation, was designated for real-time processing applications. The proposed technique shows excellent airborne magnetic data results considering actual field examples. The proposed technique verifies an accurate and objective tool for magnetic objects detection compared with the existing PEI tools considering cost and processing automation capabilities.

Keywords: Airborne magnetic, unexploded ordnance, parallax/Lag, air-condition, noise, microcontrollers

1. Introduction

A major problem with unexploded ordnance is that over the years the detonator and main charge deteriorate, frequently making them more sensitive to disturbance, and therefore more dangerous to handle. There are countless examples of people tampering with unexploded ordnance that is many years old often with fatal results. Believing it to be harmless they handle the device and it explodes killing or severely injuring them [1-3]. For this reason it is universally recommended that unexploded ordnance should not be touched or handled by unqualified persons. Instead, the location should be reported to the local police so that bomb disposal or Explosive Ordnance Disposal (EOD) professionals can render it safe.

The main systems on board the geophysical aircraft are magnetic, gamma ray spectrometry, electromagnetic, and gravity, which measure different physical properties of the earth [4-5]. In the case of the magnetic system, which is the point of interest within the present paper, the instrument measures the strength of the magnetic field of the earth, which provides information on the different rock types under the ground. It also allows

geologists and the geophysicists to identify different structures in the earth. Such faults or fractures are often pathways where water, mineralized fluids or radon travel through the earth [6-11].

2. Sources of Distortion and Noise on the Airborne Magnetic Data

The airborne magnetic data suffers different types of noises, which in turn affects the collected data quality. Hereinafter a brief description of such noises will be described [12-13]:

1. Air Conditioning Noise: Air condition system irregularly operates to cope with the sharp changes in the temperature of the plane during the geophysical survey, specially, over arid areas.
2. Parallax/Lag Effect: A lag effect appears due to the time takes for the sensor to move to the position of the aircraft, which is a function of the aircraft speed and the distance between the aircraft and the sensor, is known as the lag.
3. DC Shift Noise: This type of noise signature is, also, appears irregularly, the matter is due to the operation of the aircraft moving parts such as motors, ventilators, navigation systems, etc. Such noise appears to be severe, due to the continuous air-craft movements and sudden tracking of terrain, while pilots fighting to maintain to keep constant survey altitude over the survey area.
4. Heading Effect: A heading effect causes systematic shift in the data that is a function of the direction of the travel for a survey line.
5. Figure OF merit (FOM): The aircraft should be carrying out a FOM calibration flight with all on-board systems in normal operating mode. This calibration flight was made at high altitude (10,000 feet or more) over an area of subdued magnetic gradient along the sides of a rectangular box representing the principal flying directions of the survey. The net value of the FOM should be better than 1.0 nT.

This paper concerned in air conditioning noise and parallax/lag effect.

3. Design and Implementation of the Proposed Technique

This section is devoted for the selected electronic kit (EasyPIC V7) for implementing the proposed technique and also contains the major blocks of the design.

3.1. EasyPIC V7

The EasyPIC V7 is the seventh generation of the famous PIC development board (Figure1). It is the product of accumulated knowledge over the past 10 years, and it is state of the art of design, functionality and quality, where board comes with PIC18F452 device. The board can be considered so unique, as it comes with powerful on-board mikroProg programmer and In-circuit debugger, capable of programming more than 250 microcontrollers. This makes development with Easy PIC V7 a whole new experience. As well, the board has modules for all kinds of development. Beside standard DS1820 digital thermometer, LM35, analog temperature sensor was introduced. Also, Piezo buzzer was used for sound signalization and one can use 12C EEPROM to store config data. Finally, the board supports over 250 Microchip microcontrollers, and it's provided with 4-digit 7seg display, so one can build applications for LCD, GLCD and 7-Seg, all on the same board. Finally, Figure 2, shows some of the board parts.

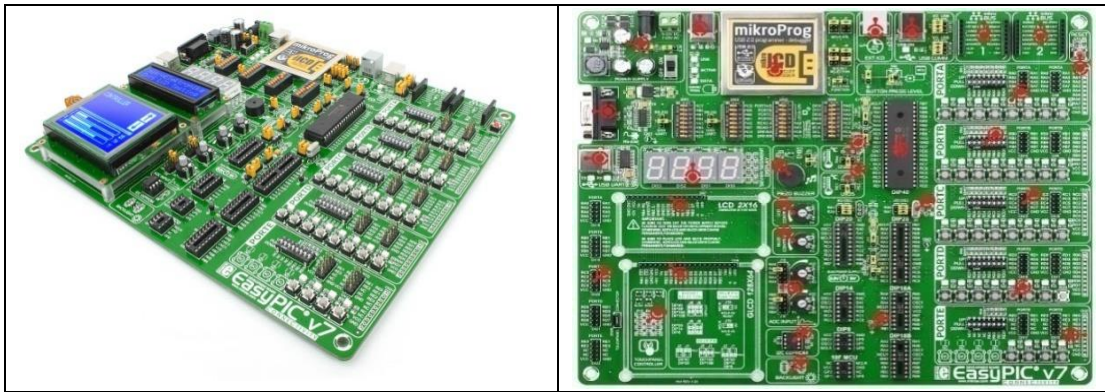
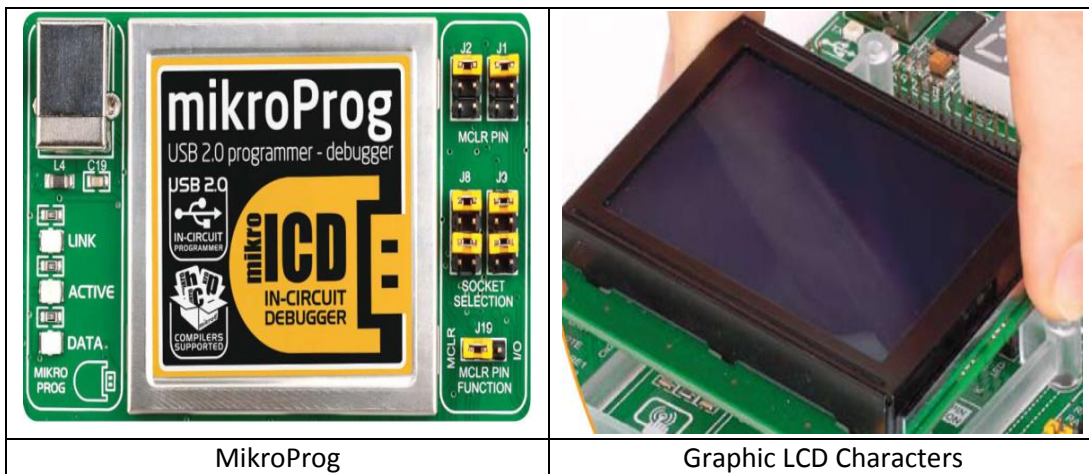


Figure 1. PIC Development Board "Easy PIC V7"



MikroProg

Graphic LCD Characters

Figure 2. Parts of Easy PIC V7 Development Board

3.2. Implementation Block Diagram

Figure 3, shows the simplest form of block diagram of the proposed system implemented on EASY PIC V7.

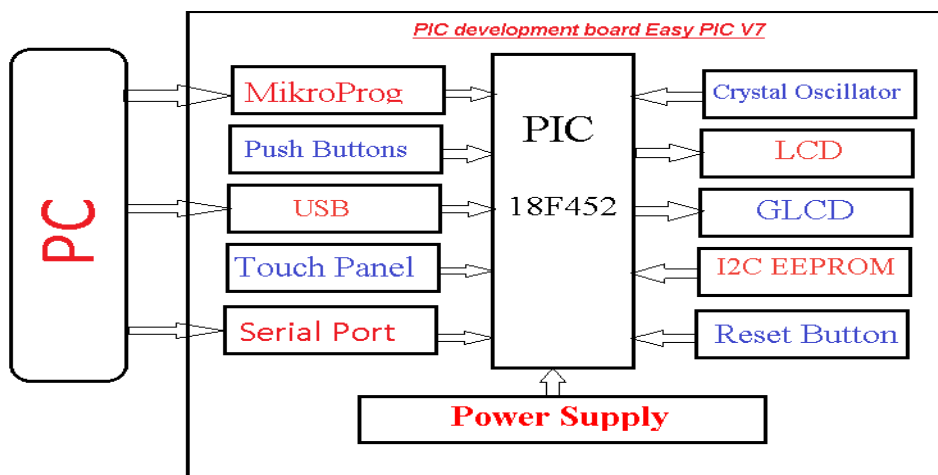


Figure 3. Block Diagram of the Proposed System Implemented on Easy PIC V7

4. Applications of Implementation Technique

4.1. Parallax/Lag Correction

A lag correction corrects magnetic data for the delay between the time of measurement and aircraft position. The time it takes for the sensor during moving the aircraft, which is a function of the aircraft speed and the magnetometer processing time, is known as the lag. A lag correction subtracts the lag (in fiducially) from the start fiducially of the data channel in the data base. Figure's(7and 8), show the flow chart of the parallax/Lag correction and the magnetic data of certain body collected on certain direction (a), its reverse direction (b), and the magnetic data of same body, collected from the two inverse directions, plotted on the same graph (c). In this concern, hereinafter a brief mathematical model, flowchart and description of the steps applied.

The first step of the work is based on the determination of the maximum magnetic field positions (max_{x_1} and max_{x_2}) for the two opposite flying directions (x_1 and x_2). Hence, the average value of the lag between the locations of any magnetic anomaly, whenever detected by the same system on two opposite directions is given as:

Where: max_{x_1} : maximum value magnetic data at certain direction,
 max_{x_2} : maximum value magnetic data at reverse direction, and
 $value_{lagx}$: value of lag position at both directions.

$$if (max_{x_2} > max_{x_1}) value_{lagx} = \left(\frac{max_{x_2} - max_{x_1}}{2} \right) \text{ else } value_{lagx} = \left(\frac{max_{x_1} - max_{x_2}}{2} \right) \quad (1)$$

Figure 4 shows Pseudo code of the parallax / lag correction.

i	: count number of variable.
p	: maximum number of data.
x_1	: position magnetic data at certain direction.
x_2	: position magnetic data at reverse direction.
max_{x_1}	: maximum position magnetic data at certain direction.
max_{x_2}	: maximum position magnetic data at reverse direction.
v_{x_1}	: value magnetic data at certain direction.
v_{x_2}	: value magnetic data at reverse direction.
max_{vx_1}	: maximum value magnetic data at certain direction.
max_{vx_2}	: maximum value magnetic data at reverse direction.
1.	START
2.	INPUT p, $x_1(0 \dots p)$, $v_{x_1}(0 \dots p)$, $x_2(0 \dots p)$, $v_{x_2}(0 \dots p)$
3.	INITIAL $i=0$, $max_{x_1}=0$, $max_{vx_1}=0$
4.	WHILE ($i < p$)
5.	IF ($max_{vx_1} < v_{x_1}(i)$) THEN
6.	$max_{vx_1} = v_{x_1}(i)$
7.	$max_{x_1} = x_{x_1}(i)$
8.	ENDIF
9.	$i=i+1$
10.	ENDWHILE
11.	INITIAL $i=0$, $max_{x_2}=0$, $max_{vx_2}=0$
12.	WHILE ($i < p$)
13.	IF ($max_{vx_2} < v_{x_2}(i)$) THEN
14.	$max_{vx_2} = v_{x_2}(i)$
15.	$max_{x_2} = x_{x_2}(i)$
16.	ENDIF
17.	$i=i+1$

```

18. ENDWHILE
19. If( $max_{vx2} > max_{vx1}$ ) THEN
20.  $value_{lagx} = (max_{x2} - max_{x1})/2$ 
21. ELSE
22.  $value_{lagx} = (max_{x1} - max_{x2})/2$ 
23. ENDIF
24. WHILE(i < p)
25. IF ( $max_{vx2} > max_{vx1}$ ) THEN
26.  $x_1(i) = x_1(i) + value_{lagx}$ 
27.  $x_2(i) = x_2(i) - value_{lagx}$ 
28. ELSE
29.  $x_1(i) = x_1(i) - value_{lagx}$ 
30.  $x_2(i) = x_2(i) + value_{lagx}$ 
31. ENDIF
32. i=i+1
33. ENDWHILE
34. END

```

Figure 4. Pseudo Code of the Parallax / Lag Correction

After show the mathematical model and pseudo code, the second stage is data Processing; in this stage there are steps:

Step 1: Read data from PC

Figure 5, will show the real code which applied on kit.

```

for(i=0; i<p;i++)
{
if (Usart_Data_Ready())
{
vx1 [i] = Usart_Read();
x1 [i] = Usart_Read();
vx2 [i] = Usart_Read();
x2 [i] = Usart_Read();
if(maxvx1 < vx1(i))
{
maxvx1 = vx1(i);maxx1 = i;
}
if(maxvx2 < vx2(i))
{
maxvx2 = vx2(i);maxx2 = i;
}
}
}
}

```

Figure 5. Code of Read Data from PC by Serial Port

Step 2: Show Magnetic Data on GLCD

Figure 6, shows code of Graphic-LCD which is showing data on it.

```

Glcd_Dot: function draw point by two axis in GLCD
- for( i=0; i<(p -1); i++) { Glcd_Dot(i,vx1 [i], 0); }
- for( i=0; i<(p -1); i++) { Glcd_Dot(i,vx2 [i], 0); }
- for( i=0; i<(p -1); i++) { Glcd_Dot(i,vx1 [i], 0); Glcd_Dot(i,vx2 [i], 0); }

```

Figure 6. Code of Showing Magnetic Data on GLCD

Figure (7 through 9), show the magnetic data collected from flying on certain direction, its opposite direction, and on collective presentation respectively.

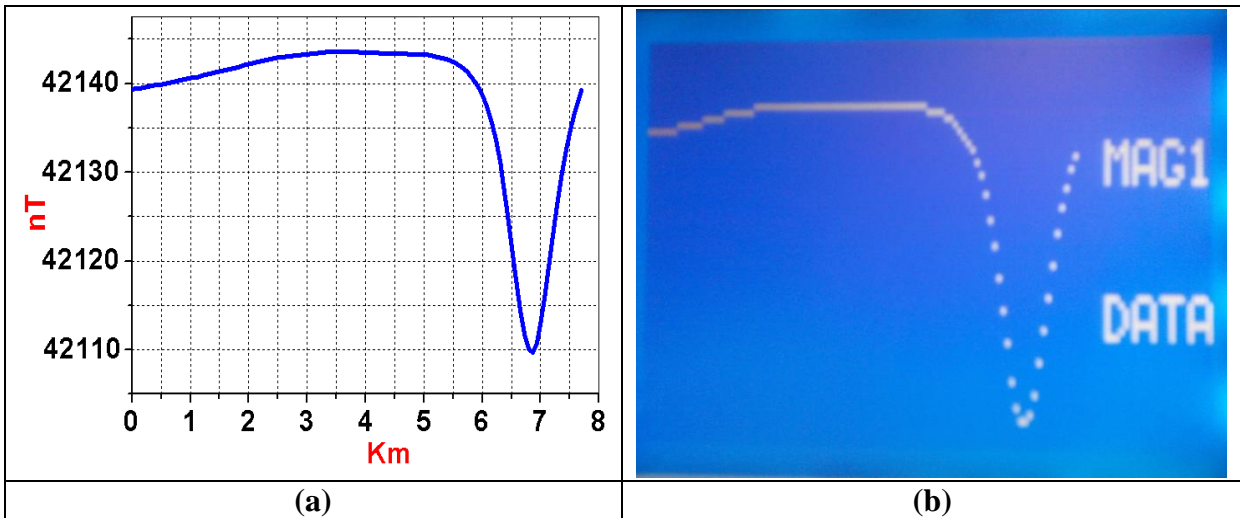


Figure 7. Magnetic Data Collected from Flying on Certain Direction (a) and PIC Display Image (b)

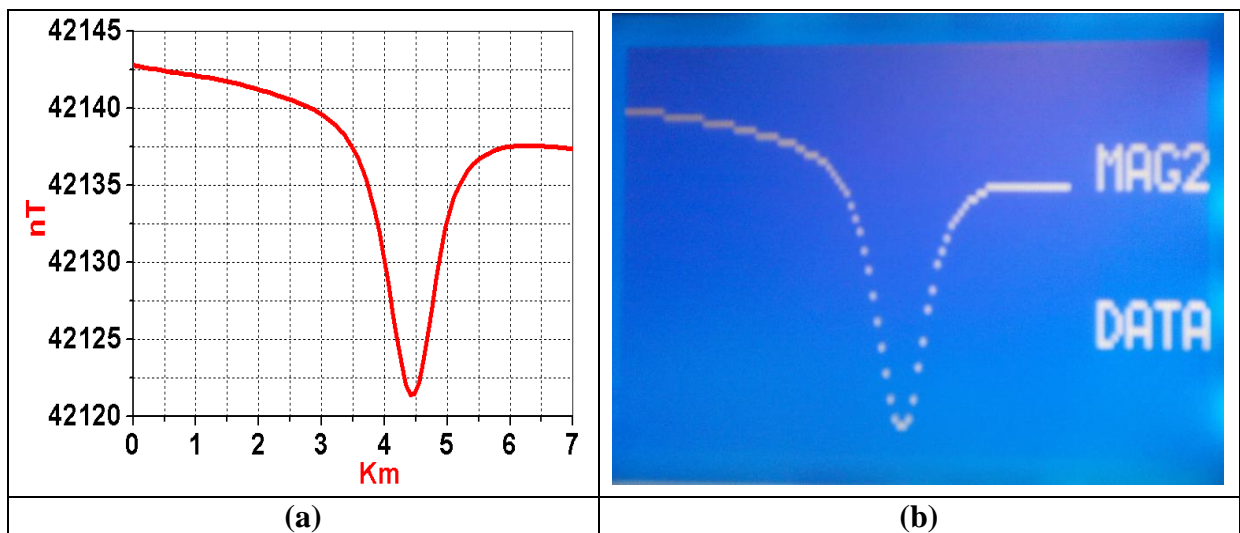


Figure 8. Magnetic Data Collected from Flying on Opposite Direction (a) and PIC Display Image (b)

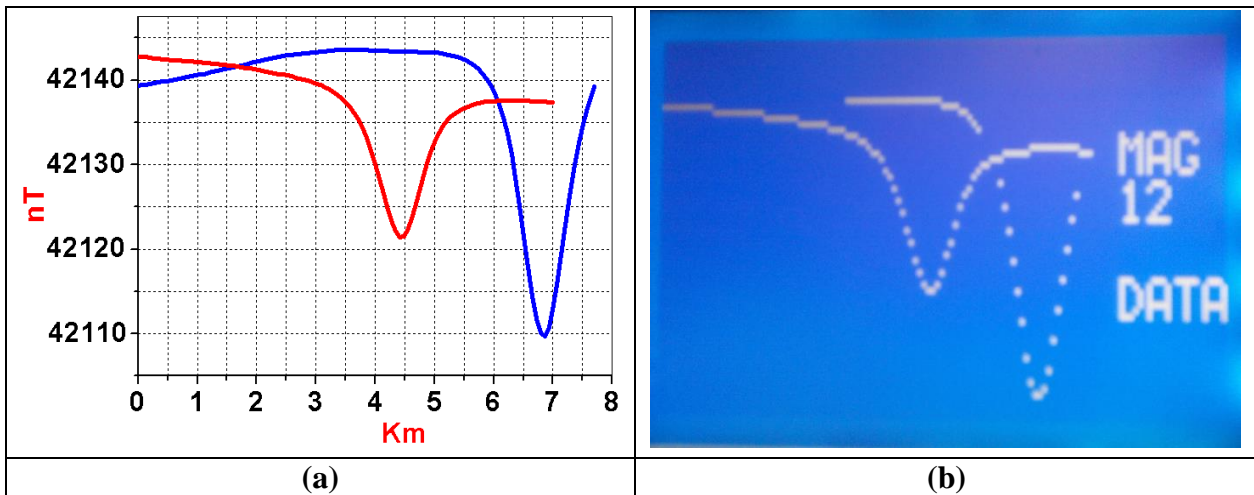


Figure 9. Magnetic Data Collected from Flying on Collective Presentation (a) and PIC Display Image (b)

Step 3: Corrections

To show the code at this step in Figure 10, which is showing the real code applied on kit.

```

-   if (maxvx2 > maxvx1 )valuelagx =( maxx2 - maxx1)/2;
-   else   valuelagx =( maxx1 - maxx2)/2;
-   for(i=0;i<p;i++)
-   {
-       if(maxvx2 > maxvx1)
-       {
-           X1(i)= x1(i) + valuelagx
-           X2(i) = x2(i) - valuelagx
-       }
-       else
-       {
-           X1(i)= x1(i) - valuelagx
-           X2(i) = x2(i) + valuelagx
-       }
-   }

```

Figure 10.Code of Processing Data.

Step 4:Show data on GLCD

Figure 11, shows the code, which applied on Graphic LCD to show filter data

```

-   for( i=0; i<(p -1); i++) { Glcd_Dot(i,vx1 [i], 0);          }
-   for( i=0; i<(p -1); i++) { Glcd_Dot(i,vx2 [i], 0);      }
-   for( i=0; i<(p -1); i++) { Glcd_Dot(i,vx1 [i], 0); Glcd_Dot(i,vx2 [i], 0); }

```

Figure 11.Code of Showing Filter Data

Figure (12 through 14), show the magnetic data collected after applying lag correction on certain direction, its opposite direction (a), and on collective presentation respectively.

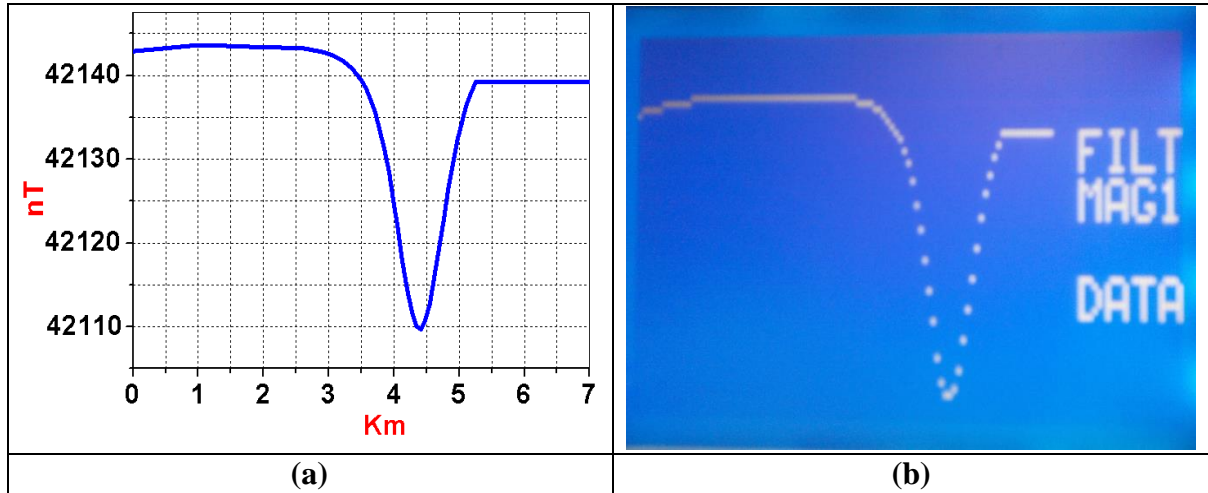


Figure 12. Magnetic Data Collected after Applying Lag Correction on Certain Direction (a) and PIC Display Image (b)

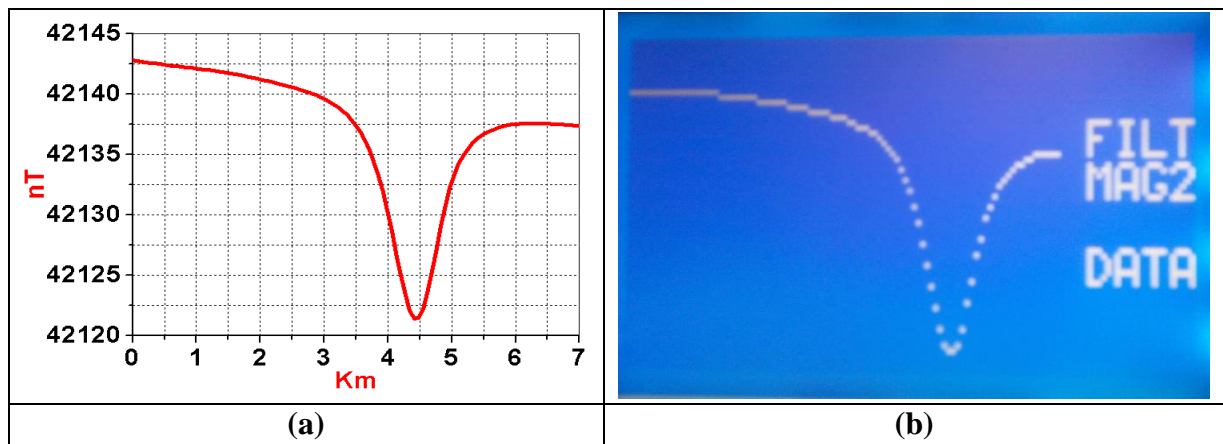


Figure 13. Magnetic Data Collected after Applying Lag Correction on Opposite Direction (a) and PIC Display Image (b)

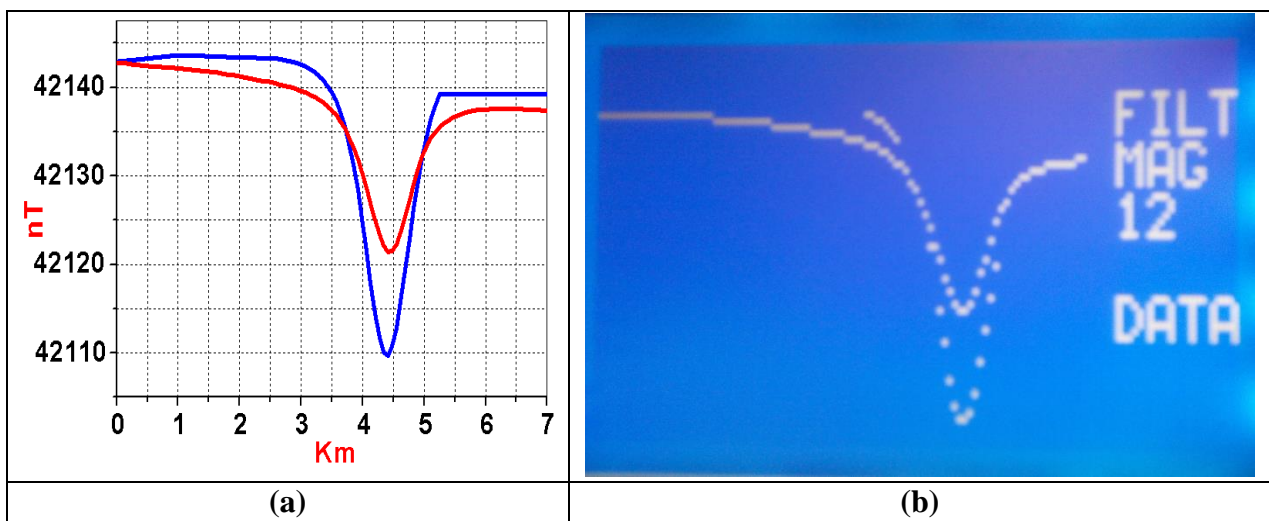


Figure 14. Magnetic Data Collected after Applying Lag Correction on Collective Presentation (a) and PIC Display Image (b)

4.2. Air Condition Noise Correction

The source of airborne magnetic data noise is due to the air-conditioning system installed onboard the aircraft. Where, air condition systems irregularly operate to cope with the sharp changes in the temperature of the plane during the geophysical survey, specially, over arid areas. As a result, an effective noise signal appears (shown as red circles; Figure15), during the irregular switching ON and OFF cycles of the air-conditioning system, to be superimposed the magnetic signature. So, the present part of the paper was mainly concerned with the accurate determination and correction of the air condition noise due to the operation of air condition installed on board the aircraft during magnetic survey. In this concern, hereinafter a brief mathematical model, flowchart and description of the steps applied.

Figure 15, shows the Air-condition noise superimposed airborne magnetic data over certain flight line (a), true noise segment (b), and PIC display image (c).

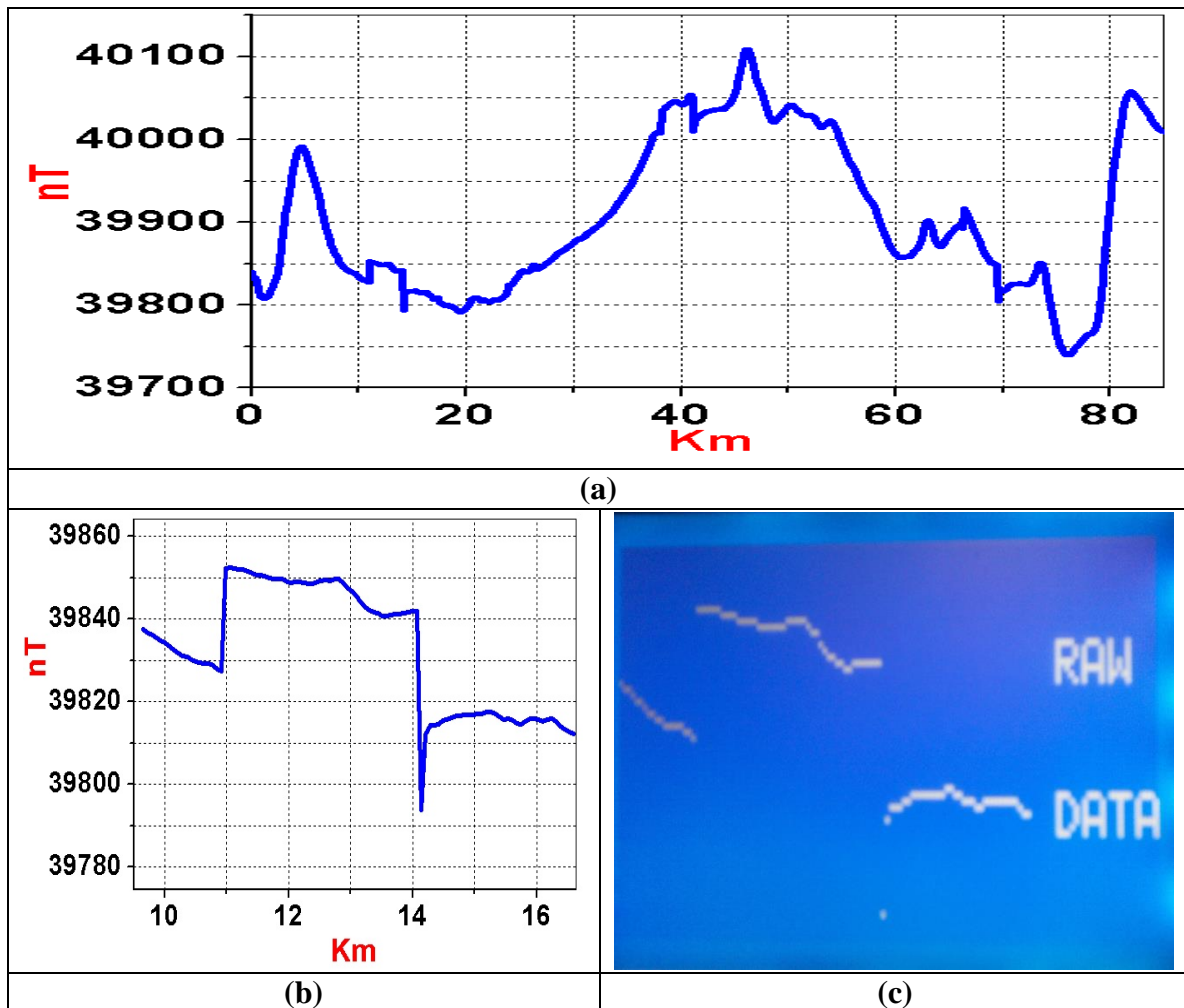


Figure 15. Air-Condition Noise Superimposed Airborne Magnetic Data Over Certain Flight Line (a), True Noise Segment (b), and PIC Display Image (c)

To filter data there are some questions such as, is there noise, if yes how program determine it. To answer these question by the next equations (2 through 7):

where : mag : raw data,
 mag_{diff} : data after fourth differential

$start_{shift_air}$: coordinate of start interval noise shift air,
 end_{shift_air} : coordinate of end interval noise shift air,
 $count_{shift_air}$: difference coordinate of interval noise shift air,
 $step_{shift_air}$: step value magnetic data which added to raw data to remove noise,
 $total_{shift_air}$: total value magnetic data which added to raw data to remove noise,
 and
 $filter_{data}$: magnetic data after filter from air condition noise.

$$mag_{4_diff}[n] = \sum_{n=1}^{n=p-1} (mag[n-4] - (4 * mag[n+2]) + mag[n-2] + (6 * magp[n]) + mag[n-4])/16 \quad (2)$$

$$if ((mag_{4_diff}[n-1] > mag_{4_diff}[n]) \text{ and } (mag_{4_diff}[n] > 2)) \text{ then} \quad (3)$$

$$count_{shift_air} = end_{shift_air} - start_{shift_air} \quad (4)$$

$$step_{shift_air} = raw_{data}[end_{shift_air}] - raw_{data}[start_{shift_air}] \quad (5)$$

$$total_{shift_air} += step_{shift_air} \quad (6)$$

$$filter_{data}[n] = raw_{data}[start_{shift_air}][n] + total_{shift_air} \quad (7)$$

Figure 16, will show pseudo code of processing data.

```

1. START
2. INPUT p, raw_data(0 ... p)
3. INITIAL m=0
4. WHILE(m < p)
    fourth_different_filter_data(m) = get_fourth_different_data(raw_data(m))
    m = m + 1
5. ENDWHILE
6. INITIAL s= 4, start_air_condition=1
7. IF (fourth_different_filter_data(s) > start_air_condition) THEN
    fourth_different=0
    start_1_shift_air=end_1_shift_air= 0
    start_2_shift_air=end_2_shift_air =0
    index_array =count_shift_air=total_shift_air=0
    GOTO 9
    ELSEIF
    Filter_data(s) = raw_data(s)
8. ENDIF
9. INITIAL j=s
10. fourth_difference = get_fourth_different_data(raw_data(j))
11. IF (fourth_difference < start_shift_air ) THEN
    count_shift_air = count_shift_air + 1
12. ENDIF
13. IF (end_1_shift_air = 0) THEN
14.     end_1_shift_air = j
15.     count_shift_air = count_shift_air + 1
16. ENDIF
17. end_2_shift_air= j
18. count_shift_air = count_shift_air + 1
19. j = j +1
20. IF ( j > ( index_array+50) ) THEN
21.     GOTO 10
22. ENDIF
23. IF (count_shift_air > 25) AND (end_2_shift_air > 0) AND (end_1_shift_air > 0) THEN
24.     step_shift_air = (raw_data(end_2_shift_air + 2) - raw_data(start_shift_air -1)) / (count_shift_air + 1)
    
```

```
25.    s= s
26. total_shift_air = total_shift_air + step_shift_air
27. filter_data (S) = raw_data(start_shift_air -1 ) + total_shift_air
28.    s = s+ 1
29.    IF ( s > end_2_shift_air) THEN
30.        GOTO 26
31.    ENDIF
32.    IF ( s <p) THEN
33.        GOTO 7
34.    ENDIF
35. ELSE
36.    GOTO 10
37. ENDIF
38. STOP
```

Figure 16.Pseudo Code of Processing Data

After seeing the equations and pseudo code, the next stage implementation at kit. This stage consist of steps:

Step 1: Read data from PC (serial port or USB):

```
- For(i=0; i<p; i++)
- {
-     if (Usart_Data_Ready())
-     {
-         raw_data [i] = Usart_Read();
-     }
- }
```

Figure 17.Code of Read Data

Step 2: Show Air-condition Noise in Magnetic Data on GLCD

```
- for(i=0;i<(P -1);i++) { Glcd_Dot(i, raw_data[i], 0); }
```

Figure 18.Code of Show Data

Step 3: Get Fourth Different Data:

```
- for(i=0; i<p; i++)
- {
-     fourth_different [i]= (raw_data [i+4]- (4*( raw_data[i+2] + raw_data [i-2]))+ (6*
raw_data [i]) + raw_data [i -4])/16.0;
- }
```

Figure 19.Code to Get Fourth Different of Raw Data.

step 4: Show Fourth Different Data on GLCD

```
- for(i =0; i<P; i++) { Glcd_Dot(i, fourth_different [i], 0); }
```

Figure 20.Code to Show Fourth Different of Raw Data.

Figure 21, shows the Airborne magnetic data after fourth differential processing (Figure21a), true noise segment (Figure21b), and PIC display image (Figure 21c).

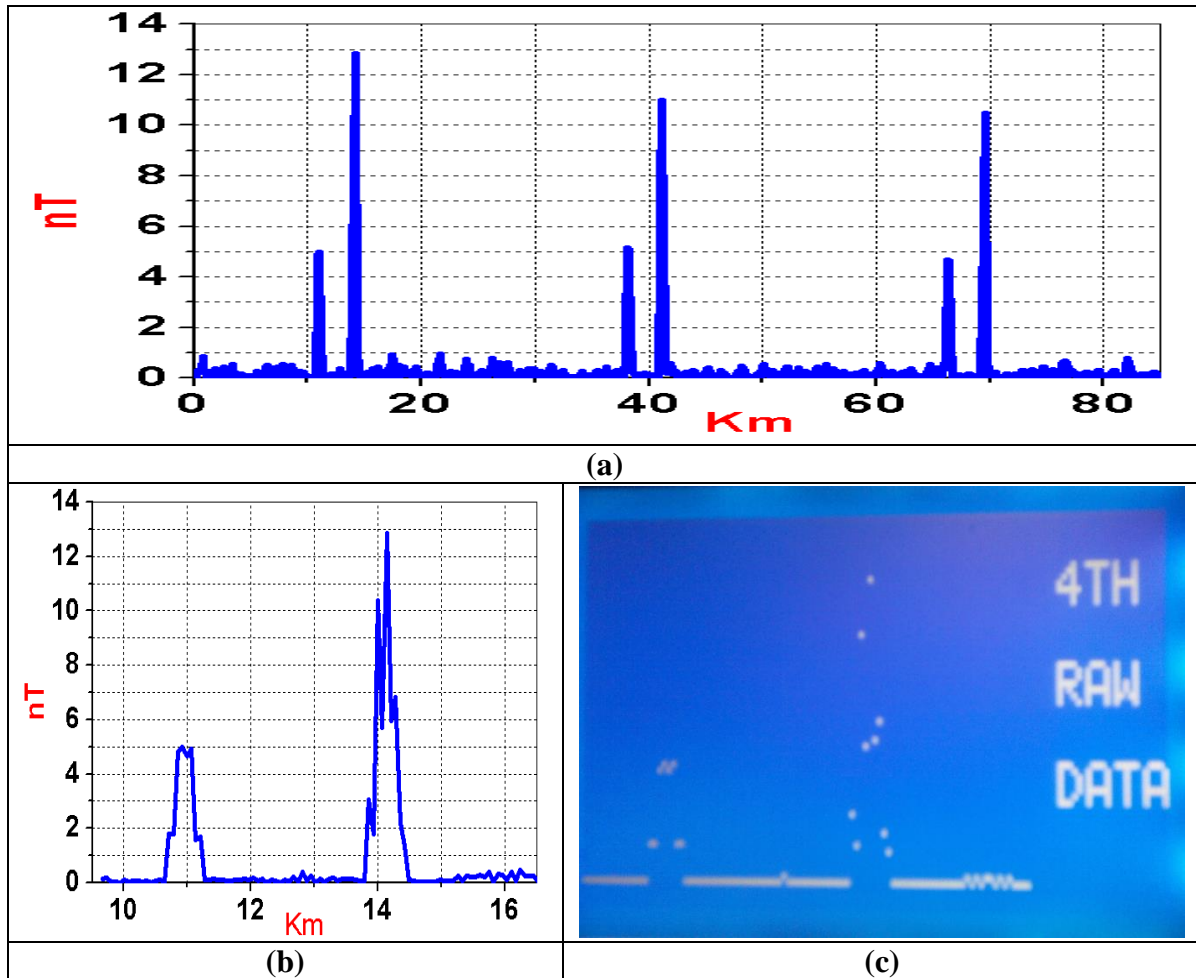


Figure 21. Airborne Magnetic Data after Fourth Differential Processing (a), True Noise Segment (b), and PIC Display Image (c)

Step 5: Determination of the start and end of noise signal

```

-   for(i=4; i<max_data; i++)
-   {
-   start_shift_air = end_shift_air = 0;
-   if ( fourth_different [i ] > 1.0 )
-   {
-   start_shift_air = i;
-   i = i +6;
-   while(end_shift_air == 0)
-   {
-   i = i + 1;
-   if( fourth_different [i ] > 1.0)
-   {
-   end_shift_air = i;
-   i = end_shift_air+2 ;
-   }
-   }
-   }
-   }
-   }
    
```

Figure 22. Code Determination of the Start and End of Noise Signal

Step 6: Air-condition Noise Removal

```
- total_shift_air=0;  
- start_shift_air--;  
- end_shift_air+=8;  
- count_shift_air=end_shift_air - start_shift_air;  
- step_shift_air = (filter_data[end_shift_air] - filter_data[start_shift_air]) /  
  (count_shift_air);  
- for(j=start_shift_air;j<= end_shift_air;j++)  
- {  
- total_shift_air += step_shift_air;  
- filter_data[j] = (filter_data[start_shift_air]+total_shift_air);  
- }
```

Figure 23. Code Air-condition Noise Removal

Step 7: Show Filter of Noise Data on GLCD

```
- for(i =0; i<(P-1); i++) { Glcd_Dot(i, filter_data [i], 0); }
```

Figure 24. Show Filter of Noise Data on GLCD

Figure 25, shows the net purified magnetic data obtained after removing the air-condition noise (a), true noise segment (b), and PIC display image (c).

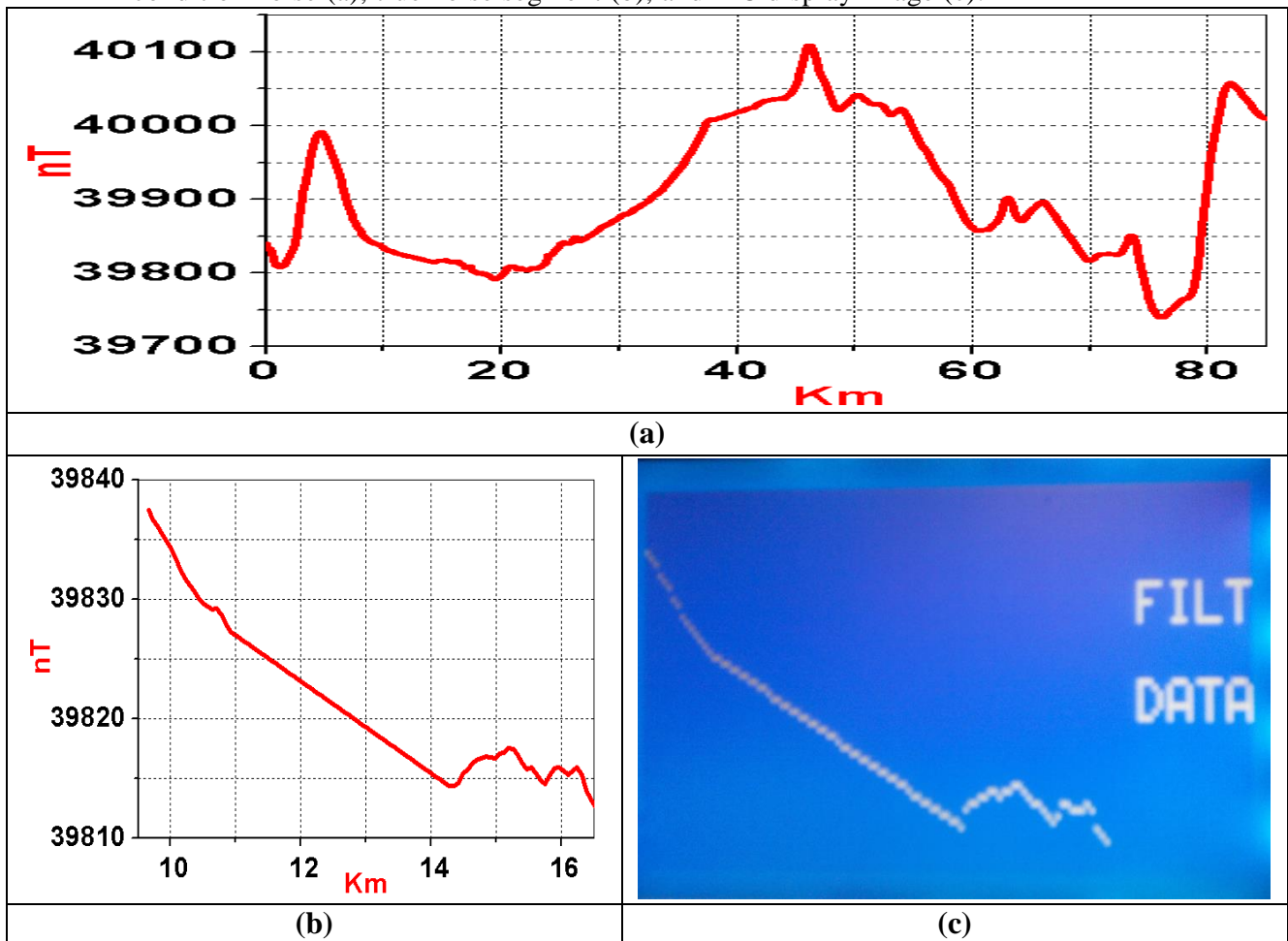


Figure 25. Net Purified Magnetic Data Obtained after Removing the Air-Condition Noise (a), True Noise Segment (b), and PIC Display Image (c)

Step 8: Data Quality Assurance

```

- for(i=0; i<P; i++)
- {
-   Filter_fourth_different[i]=(filter_data[i+4]-(4*(filter_data[i+2] + filter_data [i-
-     2]))+(6* filter_data [i]) +filter_data [i -4])/16.0;
- }
    
```

Figure 26.Code of Data Quality Assurance

Step 9: Show fourth differential of Filter data on GLCD

```

- for(i =0; i<P; i++) { Glcd_Dot(i, Filter_fourth_different [i], 0); }
    
```

Figure 27. Code Show Fourth differential of Filter Data on GLCD

Figure 28, shows the Filter airborne magnetic data after fourth differential processing (Figure28a), true noise segment (Figure28b), and PIC display image (Figure 28c).

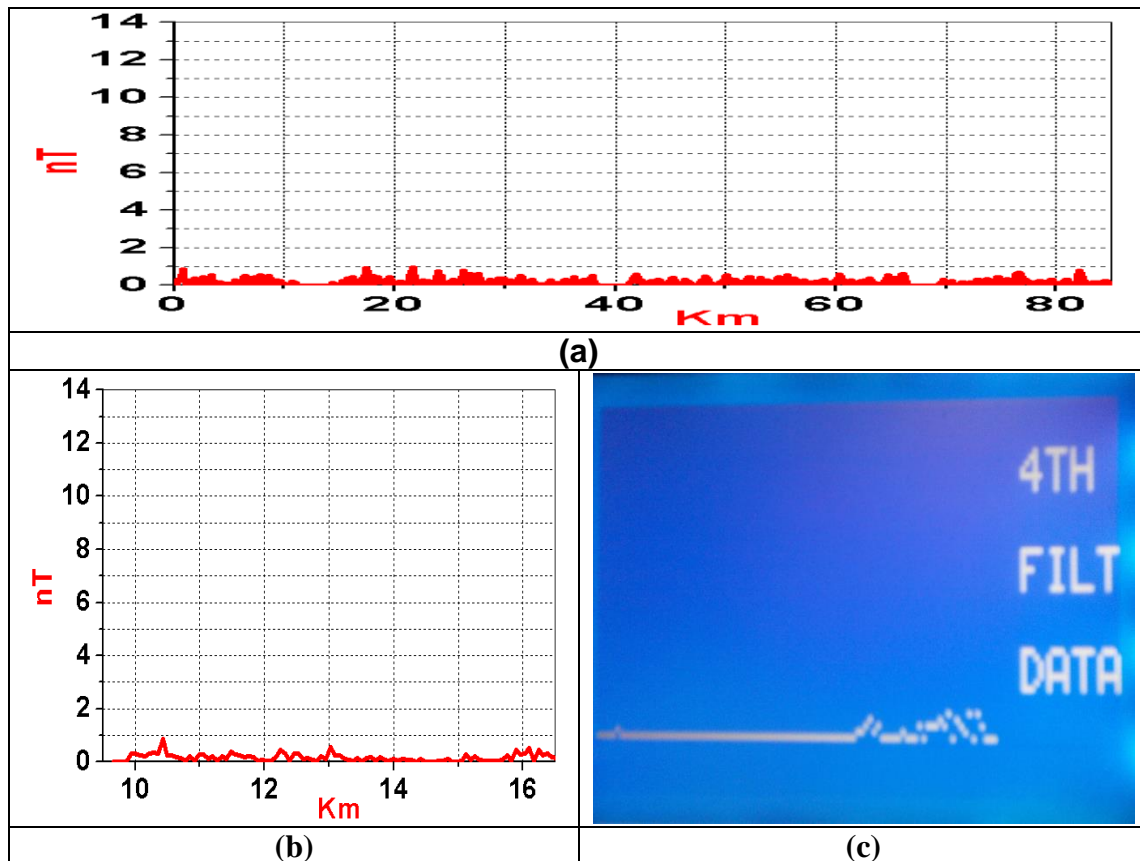


Figure 28. Filter Airborne Magnetic Data after Fourth Differential Processing (a), True Noise Segment (b), and PIC Display Image (c)

Table (1), illustrates the start and end of the noise signal obtained either theoretically or experimentally applying the proposed implementation technique. From which, it is clear that a close agreement was proved. Table (2), illustrates the obtained start and end values of the air condition noise, calculated for air borne flight line after processing.

Table (1). Theoretical and Experimental Data of the Start and End Values of Air Condition Noise

Noise No.	Start			End		
	data number	Value theoretical	Value practical	data number	Value theoretical	Value practical
1	157	5.00437	5.003662	203	12.84513	12.84399
2	546	5.17500	5.174072	589	11.01344	11.01269
3	948	4.68962	4.689941	994	10.49481	10.49365

Table (2). Theoretical and Experimental Data of the Start and End Values of Air Condition Filter

Noise No.	Start			End		
	data number	Value theoretical	Value practical	data number	Value theoretical	Value practical
1	157	0.009	0.00292	203	0.0	0.000244
2	546	0.0021	0.00268	589	0.0	0.001953
3	948	0.094	0.09448	994	0.0	0.001464

5. Conclusions

This paper introduces a new electronic processing technique for accurate detection and correction of unexploded ordnance. The proven tools include mathematical analysis, design and implementation. The performance of the measured data, practical applications, field correction capabilities and analysis verifications are the used tools to verify that the measured results confirm the theoretical analysis. The selected applications for implementation are real-time correction of parallax/lag and air condition noises in airborne magnetic data acquisition, based on microcontrollers. These applications are considered to be of great rule for accurate detection of unexploded ordnance.

References

- [1] Wikipedia, "Unexploded Ordnance", en.wikipedia.org/wiki/Unexploded_Ordnance. https://en.wikipedia.org/wiki/Unexploded_Ordnance.
- [2] M. Lambert, "Unexploded Ordnance: A Reference Guide for the Citizen", Environmental Science and Technology Briefs for Citizens, Kansas State University www.engg.ksu.edu/HSRC/Tosc/uxo.pdf
- [3] M. N. Nabighian, V. J. S. Grauch, R. O. Hansen, T. R. LaFehr, Y. Li, J. W. Peirce, J. D. Phillips and M. E. Ruder "Geophysics Today: A Survey of the Field as the Journal Celebrates Its 75th Anniversary" Society of Exploration Geophysicists, (2010), pp. 183-213.
- [4] B. Howard, J. Aker, M. Reid "Risk Management For Unexploded Ordinance (UXO) In The Marine Environment", vol 8, no. 2, (2012).
- [5] K. Davis, Y. Li and M. Nabighian "Automatic detection of UXO magnetic anomalies using extended Euler deconvolution", vol. 75, (2010).
- [6] E. Camara and S.Guimares "Magnetic airborne survey-geophysical flight", Geoscientific Instrumentation Methods on and Data systems, vol. 5, June (2016), pp. 181-1192.
- [7] PicoEnvirotec, Inc., www.picoenvirotec.com/.
- [8] M. El-kattan, H. El-Henawy, A. D. Kamal, F. A. S. Soliman, A. Salem and A. Osman, "Integrated detection of landmines using neutron back-scattering and magnetic gradient techniques", 22nd Intr. Geophysical Conf. and Exhibition, Brisbane, Australia, (2012) February 26-29.
- [9] M. El-Kattan, A. Salem, F. A. S. Soliman, A. D. Kamel, H. El-Hennawy, "Microcontroller based neural network for landmine detection using magnetic gradient Data", 4th Intr. Conf. on Intelligent and Advanced Systems, ICIAS2012, Kuala Lumpur, Malaysia, (2012) June, 12-14 pp. 46-50.
- [10] K. Davis, Y. Li and M. Nabighian "Automatic detection of UXO magnetic anomalies using extended Euler deconvolution", vol. 75, (2010).
- [11] M. Elkattan and M. Elsayed "Detection of Landmines Using Innovative Technologies", Ph.D. Thesis, Faculty of Engineering, Ain-Shams University, Cairo, Egypt, Nuclear Materials Authority, P.O.Box 530, Maadi-11728, Cairo, Egypt, (2013).

- [12] M. Abdel-Maksood, "Electronic Implementation of Hopfield Neural Network for Depth Determination of Buried Ferro-Metallic Objects", Ph.D. Thesis, Faculty of Engineering, Al-Azhar University, Cairo, Egypt., Nuclear Materials Authority, P.O.Box 530, Maadi-11728, Cairo, Egypt, (2011).
- [13] A.S.S.El-Kabbani, K.G. Abdel-Kader, A.A.M.Ismail, F.A.S.Soliman, and A.M.Abdel-Maksoud, "Design and Application of an Automatic Technique for Maneuvers Correction of airborne Magnetic Data", Egyptian Geophysical Society, EGS., vol. 12, no. 1, (2014) January, pp. 113-121.

Authors



Fouad A. S. Soliman, Professor of Electronics and computers Eng., Nuclear Materials Authority of Egypt. Member of American Assoc. for Adv. of Sci's., N.Y., U.S.A and New York Academy of Sciences, New York, U.S.A. Editorial Board Member of: Progress in Photovoltaics "Research and Applications", John Wiley and Sons, UK, Periodicals of the Assoc. for Adv. of Modeling and Simulation Tech's., AMSE, Lune, France, Intr. Journal of Computer Sci. and Eng. Applications (IJCSEA). Chosen For: Who's Who in the World, A.N. Marquis, N.J., USA, and Outstanding People of the 20th Century, Intr. Biographical Center of Cambridge, England. Published three Books at Lambert Academic Publi-shing, LAP, Saarbrücken, Germany, ISBN 978-3-659-83496-7, ISBN 978-3-659-88129-9, and "ISBN 978-3-659-89387-2
Email:fouad.saad.soliman@gmail.com



Atef Ali Mahmoud Ismail Elshayat, Professor of Applied and Exploration Geophysics, Head of Airborne Geophysics Department, Exploration Division, Nuclear Materials Authority (NMA). Share in Computerized Database for Mineral Exploration and Development for Uranium in Particular, Zambia. Airborne Surveying Techniques, Field Operations and Data Handling Procedures. OASIS Montaj for Airborne Geophysics GEOSOFT, Canada. Work on Airborne Gamma-Ray Spectrometer System, East China Institute of Technology, Nanchang, Fouzou, China. Member for calibration, operation & maintenance of advanced airborne geophysical instrumentation system, Pico Envirotec Inc., Ontario, Canada.

E-mail:elshayatatef@yahoo.com



Ahmed Yahya has received Ph.D. degree in Electronics and Communication Engineering from Ain Shams University in 1998. He has a teaching experience at both the under graduate (UG) and the post graduate (PG) levels. Currently, he is an Associate Professor with the Department of Electrical Engineering, Faculty of Engineering, Al-Azhar University, Cairo, Egypt. His areas of interest include nan electronic & low noise amplifier circuit design, IOT etc.

Email:ahmed_yahya_1@yahoo.com



Ashraf Mosleh Abd El-Maksood, Lecturer of Electronics Engineering, Electronics Eng. Dept., Nuclear Materials Authority of Egypt. Major field of interest: Energy, Electronics, Radiation detection and computer programming and simulation.

Email:ashrafmosleh1@gmail.com



Khaled Gamal Abd-kader, Electrical engineer, South Cairo Electricity Distribution Co., Ministry of Electricity and Renewable Energy. Power electronic designer. Embedded system programmer.
Email:khasdasd2000@gmail.com

